Temperature independent 80 Gb/s transmission system using spectral phase modulation-based TDC

Kangping Zhong (钟康平)[1,2*], Tangjun Li (李唐军)[1,2], Nan Jia (贾 楠)[1,2], Jian Sun (孙 剑)[1,2], and Muguang Wang (王目光)[1,2]

[1]*Key Laboratory of All Optical Network and Advanced Telecommunication Network of EMC, Beijing Jiaotong University, Beijing 100044, China*

[2]*Institute of Lightwave Technology, Beijing Jiaotong University, Beijing 100044, China*

[*]*Corresponding author: 09111023@bjtu.edu.cn*

Received April 15, 2011; accepted July 12, 2011; posted online September 27, 2011

A temperature independent 80-Gb/s 100-km transmission system is demonstrated with the use of spectral phase modulation-based tunable dispersion compensator (TDC). The principle of dispersion compensation based on spectral phase modulation as well as the relationship between spectral phase modulation function and group velocity dispersion (GVD) are theoretically studied. TDC based on spectral phase modulation is implemented. The performance of 80-Gb/s transmission system is experimentally evaluated. The nonlinear relationship between temperature and temperature-induced dispersion fluctuations is demonstrated through the asymmetric temperature-induced power penalty without dispersion compensation. With respect to the low temperature area, the temperature-induced dispersion fluctuations are smaller than those in the high temperature area. By using the proposed TDC, temperature independent 80-Gb/s transmission is successfully demonstrated under a temperature range of –20 – 60 °C with a power penalty of less than 0.8 dB.

OCIS codes: 060.4230, 060.2360, 060.2330, 060.4510, 060.5060.

doi: 10.3788/COL201210.020602.

In recent years, with the growing demand for wideband communication systems, high bit rate (>40 Gb/s) transmission systems have attracted considerable attention. However, the introduction of high speed increases the impairment of data channels due to chromatic dispersion[1], polarization mode dispersion (PMD)[2], and nonlinearities[3]. Chromatic dispersion is a critical impairment that limits system performance. Moreover, dispersion fluctuations introduced by environmental changes such as temperature variations should be considered. Moreover, tunable dispersion compensation is a prerequisite in the design of high-speed transmission systems due to its tight dispersion tolerance.

This issue has been extensively studied in recent years. André *et al.* pointed out that systems with 40 Gb/s or higher bit rates suffer serious impairments due to temperature-induced dispersion fluctuations, thus requiring tunable dispersion compensation[4]. One possibility of controlling the temperature of the dispersion compensating fiber (DCF) to dynamically compensate for the chromatic dispersion fluctuations induced by the environmental temperature alterations is presented[5]. However, in practical optical communication systems, DCF is a part of the transmission link buried underground together with G.652 fibers. Hence, it is impractical to control the temperature of DCF. Bourdoucen proposed a method to compensate for the temperature dispersion effect by adjusting the length of DCF[6]. However, the method is too complicated to be implemented in an installed fixed transmission link. Hirano *et al.* implemented a temperature independent transmission system using a zero-dispersion flattened transmission line[7]. However, the method used is dependent on specific fibers to form the zero-dispersion flattened transmission line.

In this letter, we demonstrate a temperature independent 80-Gb/s transmission system using spectral phase modulation-based tunable dispersion compensator (TDC). We theoretically study the principles of compensating dispersion based on spectral phase modulation technology. A TDC with a tunable range of –40 – 40 ps/nm based on spectral phase modulation is implemented. The effects of dispersion fluctuations due to temperature variations over a range of –20 – 60 °C, in 80-Gb/s optical time domain multiplexing (OTDM) transmission system are evaluated in experiments using eye-diagrams and BER performance. With tunable dispersion compensation, temperature independent 80 Gb/s was realized over a range of –20 – 60 °C. The power penalty is less than 0.8 dB.

In this letter, a simplified non-linear Schrödinger equation which neglects attenuation, high-order dispersion, fiber nonlinearity, and PMD, is given to assess the effects of chromatic dispersion in high-speed optical communication systems:

$$(-\mathrm{i})\frac{\partial u}{\partial z} = \frac{\beta_2}{2}\frac{\partial^2 u}{\partial T^2}. \tag{1}$$

Equation (1) is solved using the Fourier transform method. We obtain the transmitted signal as

$$u(z,T) = \frac{1}{2\pi}\int U(z,\omega-\omega_0)\exp[-\mathrm{i}(\omega-\omega_0)T]\mathrm{d}(\omega-\omega_0), \tag{2}$$

where ω_0 is the radian frequency at center wavelength of the signal and $U(z,\omega-\omega_0)$ is the Fourier transform of

the signal at z, whose solution is given as

$$U(z,\omega-\omega_0)=U(0,\omega-\omega_0)\exp\left[\frac{\mathrm{i}}{2}\beta_2(\omega-\omega_0)z\right], \quad (3)$$

where $U(0,\omega-\omega_0)$ is the Fourier transform of the signal at $z=0$. Hence, the general solution of Eq. (1) is given as

$$u(z,T)=\frac{1}{2\pi}\int U(0,\omega-\omega_0)\exp\left[\mathrm{i}\frac{\beta_2}{2}z(\omega-\omega_0)^2-\mathrm{i}(\omega-\omega_0)T\right]\mathrm{d}(\omega-\omega_0). \quad (4)$$

Without dispersion compensation, the transmitted pulses would be affected by severe temporal broadening, which significantly degrades the performance of transmission systems. Equation (4) indicates that dispersion contributes a phase change in every spectral component of the signal, causing the pulse broadening to yield. In this case, the broadened pulses could be restored to their normal shape if we remove the phase change of every spectral component induced by dispersion. Thus, the addition of an appropriate spectral phase modulation to the transmitted signal will compensate for the effects of fiber dispersion. Assuming that a spectral phase modulation $\phi(\omega)$ is added to the transmitted signal, then the field of signal after spectral phase modulation is given as

$$u_c(z,T)=\frac{1}{2\pi}\int U(0,\omega-\omega_0)\exp\left[\mathrm{i}\frac{\beta_2}{2}z(\omega-\omega_0)^2+\mathrm{i}\phi(\omega)-\mathrm{i}(\omega-\omega_0)T\right]\mathrm{d}(\omega-\omega_0). \quad (5)$$

In order to cancel the additional phase variations induced by dispersion completely, we obtain

$$\phi(\omega)=-\frac{\beta_2}{2}z(\omega-\omega_0)^2. \quad (6)$$

The compensated signal will be given as

$$u_c(z,T)=\frac{1}{2\pi}\int U(0,\omega-\omega_0)\exp[-\mathrm{i}(\omega-\omega_0)T]\mathrm{d}(\omega-\omega_0)=u(0,T). \quad (7)$$

Equation (7) shows that the distorted signal is restored after spectral phase modulation. A relationship between dispersion coefficient D and phase change can be obtained from Eq. (6)

$$\phi(\lambda)=-\pi cDz\left(1-\frac{\lambda}{\lambda_0}\right)^2, \quad (8)$$

where D is the dispersion coefficient, z represents the transmission length, c is the speed of light, and λ and λ_0 are the wavelength and center wavelength of the signal, respectively. For the Dz that represents the accumulated dispersion over the whole transmission link with a unit of ps/nm, a relationship between spectral phase modulation and group velocity dispersion (GVD) could be acquired as

$$\phi(\lambda)=-\pi ca\left(1-\frac{\lambda}{\lambda_0}\right)^2, \quad (9)$$

where a is the GVD compensated by spectral phase modulation. Different GVDs can be compensated by different spectral phase modulations, which lead to the realization of tunable dispersion compensation.

Figure 1 shows the schematic overview of spectral phase modulation based TDC. The light passes through a polarization imaging optics, which changes the orthogonal polarization states to the high efficiency s-polarization state of the conventional grating. Thus, light is reflected by the imaging mirror and dispersed angularly by the grating. The dispersed light is directed by the imaging mirror into different portions of the liquid crystal on silicon (LCOS). The phase of light can be changed by adjusting the voltages on the LCOS[8]. For the wavelength channels separated on different portions of LCOS, the phase of each wavelength can be adjusted independently. A phase modulation can be realized over the entire signal spectrum. According to the relationship in Eq. (9), different GVDs can be compensated with different phase modulations. A TDC with approximately 40-nm wide operating range is realized. The compensator has the potential to compensate for dispersions simultaneously in different channels in WDM systems.

Figure 2(a) shows the spectral phase modulation $\phi(\lambda)$ for generating different GVDs from –40 to 40 ps/nm with a bandwidth of 2 nm. It was calculated by Eq. (9). The tunable characteristics of the proposed TDC are experimentally measured by CD400. Using different spectral phase modulation $\phi(\lambda)$ as shown in Fig. 2(a), different group delay curves are obtained and shown in Fig. 2(b). The results indicate that the TDC could generate different GVDs from –40 to 40 ps/nm with a bandwidth of 2 nm, which can be used to compensate for the temperature-induced dispersion fluctuations of transmission fibers in high-speed transmission systems. It should be noted that the accuracy of dispersion measurement of CD400 was not sufficient to measure

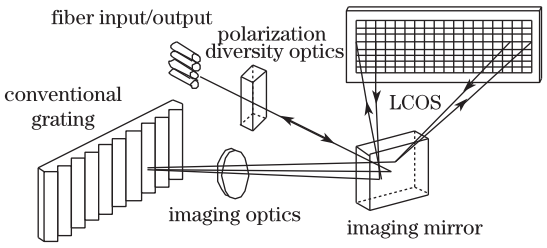

Fig. 1. Schematic overview of spectral phase modulation based TDC.

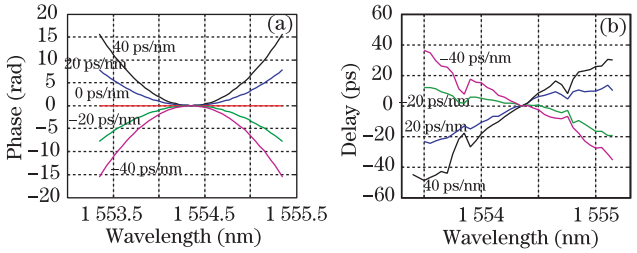

Fig. 2. Characteristics of the TDC based on spectral phase modulation for different GVDs. (a) Calculated spectral phase modulation for generating different GVDs; (b) measured GVD curves generated by TDC.

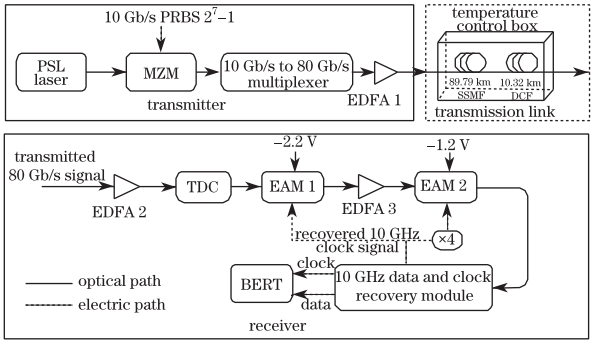

Fig. 3. Experimental setup of temperature independent 80-Gb/s 100-km transmission system. PSL: pico-second pulse laser, EAM: electro-absorption modulator.

such small GVD values. Thus, bigger group delay ripples were observed in the measured results. Nevertheless, the perfect compensation performance of the proposed TDC was revealed in a subsequent compensation experiment.

Figure 3 shows the experimental setup of temperature independent 80-Gb/s 100-km transmission system. An optical pulse train with a repetition frequency of 10 GHz is generated by a mode-locked fiber laser (PSL-10-1T, Calmar Optcom Model). The FWHM of the ultra-short pulse is shorter than 1.5 ps at a wavelength of 1 554.35 nm. Subsequently, the short pulse train is modulated by an external $LiNbO_3$ Mach-Zehnder modulator (MZM) driven by a pattern generator (Agilent N4901B) with a pseudo random bit-sequence (PRBS 2^7–1). Thus the 80-Gb/s signal is obtained by optical time multiplexing 10-Gb/s signals using homemade OTDM multiplexer[9]. The total loss of multiplexer is approximately 12 dB. Thus, the 80-Gb/s signal is powered up to 11 dBm by an EDFA and launched into a 100-km transmission link.

The 80-Gb/s OTDM signal is launched into the transmission line, which consists of three parts, namely, two spans of G.652 fibers with lengths of 46.35 and 43.44 km, and a span of DCF with a length of 10.32 km. These parts were fabricated by Yangtze Optical Fiber and Cable Company (YOFC). The total loss of transmission line is approximately 28 dB. In systems with 40 Gb/s or higher bit rates, the residual dispersion slope would degrade system performance sufficiently. Dispersion slope compensation should be considered in high-speed optical system design[10]. Therefore, the 10.32-km DCF was designed with the capacities of both compensating dispersion and dispersion slope of standard single mode fiber (SSMF) used in a transmission line. Finally, high accurate dispersion management is achieved by a 10 m level fine-tuned to compensate for both dispersion and dispersion slope, which corresponds to the accuracy of 0.4 ps for dispersion compensation[11]. All the fiber spans are placed in a temperature chamber that simulated environment temperature variations over a range of –20 °C – 60 °C.

At the receiver, an EDFA is used to compensate for the loss of the 100-km transmission line. The distorted 80 Gb/s due to temperature induced dispersion fluctuations is restored using the proposed spectral phase modulation-based TDC. Thus, the restored 80 Gb/s signal is launched into a simple loop consisting of two concatenated electro-absorption modulators (EAMs), a 10-GHz clock and data recovery module for simultaneous demultiplexing and clock recovery. The 40-Gb/s demultiplexed signal is obtained at the output of the first EAM driven by 10-GHz clock signal. An EDFA is implemented between the two EAMs to compensate for the loss of the first EAM. Moreover, because the recovery clock is set to 10 GHz, two frequency doublers are utilized to generate the 40 GHz driving signal for the second EAM. The 40-Gb/s signal was demultiplexed into 10-Gb/s signal by the second EAM and injected into the 10-GHz data and clock recovery module for clock and data recovery. Performance of this transmission system is evaluated using eye-diagrams and BER performance.

Figure 4 shows the measured eye-diagrams in different situations. Figure 4(a) presents the eye-diagrams of non-transmitted 80-Gb/s signal. The eye-diagrams of transmitted signal at temperature of 20 °C are illustrated in Fig. 4(b). The opening eye-diagrams show the perfect performance of DCF in dispersion compensation of the 89.79-km G.652 fibers at 20 °C. The eye-diagrams of the transmitted 80-Gb/s signal at different temperatures within –20 – 60 °C without tunable dispersion compensation are shown in Figs. 4(c), (e), (h), and (g). Without tunable dispersion compensation, poor quality eye-diagrams are achieved due to temperature-induced dispersion fluctuations. According to the results, dispersion fluctuations in dispersion management transmission line due to temperature variations are more severe in low temperature than in high temperature areas,

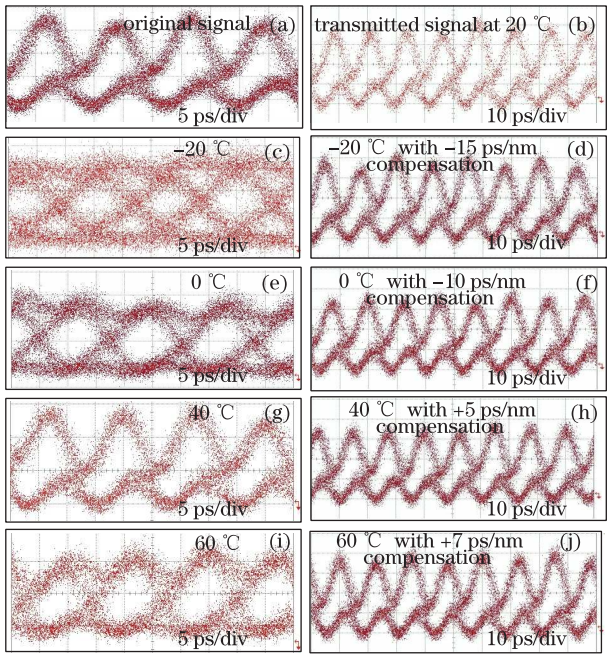

Fig. 4. (a) Eye-diagrams of measured non-transmitted 80-Gb/s OTDM signal; (b) eye-diagrams of transmitted 80-Gb/s OTDM signal at temperature of 20 °C; (c) and (d) eye-diagrams of transmitted 80-Gb/s signal at temperature of –20 °C without and with –15 ps/nm compensation; (e) and (f) eye-diagrams of transmitted 80-Gb/s signal at temperature of 0 °C without and with –10 ps/nm compensation; (g) and (h) eye-diagrams of transmitted 80-Gb/s signal at temperature of 40 °C without and with +5 ps/nm compensation; (i) and (j) eye-diagrams of transmitted 80-Gb/s signal at temperature of 60 °C without and with +7 ps/nm compensation.

indicating a non-linear temperature dependence on dispersion. With the appropriate spectral phase modulation uploaded onto our proposed TDC, different GVDs are generated to compensate for the temperature-induced dispersion fluctuations. The ASE of EDFA could be severely suppressed due to the narrow bandwidth of TDC, which is approximately 2 nm. Eye-diagrams of the transmitted 80-Gb/s signal at different temperatures with different dispersion compensations are shown in Figs. 4(d), (f), (h), and (j). The eye-diagrams are completely restored, illustrating the good performance of the proposed TDC. Finally, temperature independent error-free (BER $< 10^{-9}$) 80-Gb/s OTDM signal transmissions over 100 km are revealed over a temperature range of –20 – 60 °C. Figure 5 shows the measured receiver sensitivity (BER=10^{-9}) versus different temperatures of the 100-km transmission line with or without tunable dispersion compensation. Without dispersion compensation, a large power penalty is observed due to the temperature-induced dispersion fluctuations with respect to 20 °C. An asymmetric power penalty curve is also demonstrated. A power penalty of 5.3 dB is obtained at temperature of –20 °C without compensation, whereas approximately 1.8 dB is observed at temperature of 60 °C, with the same 40 °C temperature variation. These results reveal a non-linear temperature dependence of dispersion as illustrated by the eye-diagrams. Receiver sensitivity versus temperature with tunable dispersion compensation is also demonstrated in Fig. 5. The power penalties at different temperatures from –20 to 60 °C are demonstrated to be less than 0.8 dB with respect to 20 °C, indicating the perfect performance of proposed TDC. Figure 5 also shows the eye-diagrams of demultiplexed 10-Gb/s signal with and without compensation at –20 °C. With respect to the case without compensation, an improvement of –5.3 dB in receiver sensitivity is obtained with the tunable dispersion compensation at –20 °C. It should be noted that 1 dB improvement of

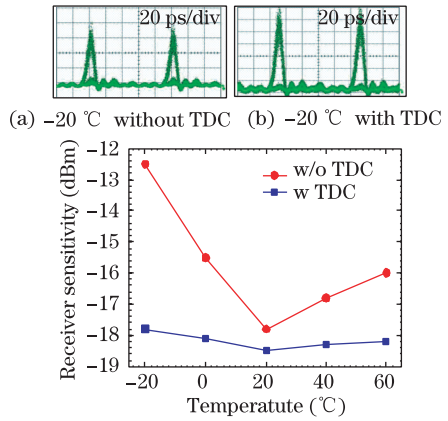

Fig. 5. Measured receiver sensitivity (BER = 10^{-9}) versus temperature without and with tunable dispersion compensation. (a) Eye-diagrams of demultiplexed 10 Gb/s without dispersion compensation at temperature of –20 °C; (b) eye-diagrams of demultiplexed 10 Gb/s with dispersion compensation at temperature of –20 °C.

receiver sensitivity demonstrated at 20 °C can be attributed to the suppression of ASE due to the narrow bandwidth of the tunable dispersion compensation (approximately 2 nm).

In conclusion, a temperature independent 80-Gb/s 100-km transmission system is demonstrated in experiments using spectral phase modulation-based TDC. A TDC with a tunable range of –40 – 40 ps/nm based on spectral phase modulation is implemented. The effects of dispersion fluctuations due to temperature variations in 80-Gb/s OTDM 100-km transmission system over a range of –20 – 60 °C are evaluated both by eye-diagrams and power penalty. Non-linear temperature dependence of dispersion is demonstrated through the asymmetric power penalty curve. Temperature induced dispersion fluctuations are more severe in low temperature area than in high temperature area. With the spectral phase modulation-based TDC, temperature independent 80 G/s is realized over a temperature range of –20 – 60 °C. Power penalties, demonstrated at different temperatures, are all smaller than 1 dB with respect to 20 °C.

This work was supported by the Fundamental Research Funds for the Central Universities, Beijing Jiaotong University (No. 2009YJS005), the National "863" Program of China (Nos. 2007AA01Z258 and 2008AA01Z15), the National Natural Science Foundation of China (Nos. 60577034, 60747002, 60837003, and 60877042), and the Beijing Nova Program (No. 2008A026). The authors would like to thank EPS Electronic Technology Ltd. for providing the spectral phase modulator (Waveshaper 4000s).

References

1. H. Ruan and C. Gan, Chin. Opt. Lett. **8,** 564 (2010).
2. F. Tian, L. Xi, X. Zhang, X. Weng, G. Zhang, and Q. Xiong, Chin. Opt. Lett. **8,** 816 (2010).
3. C. Xie, Chin. Opt. Lett. **8,** 844 (2010).
4. P. S. Andre and A. N. Pinto, Opt. Commun. **246,** 303 (2004).
5. P. S. André, B. Neto, R. Nogueira, J. L. Pinto, A. L. Teixeira, M. J. Lima, and F. Da Rocha, in *Proceedings of Lasers and Electro-Optics/International Quantum Electronics Conference and Photonic Applications Systems Technologies* CWA1 (2004).
6. H. Bourdoucen, J. High Speed Networks **1,** 51 (2008).
7. K. Yonenaga, A. Hirano, S. Kuwahara, Y. Miyamoto, H. Toba, K. Sato, and H. Miyazawa, Electron. Lett. **36,** 343 (2000).
8. M. A. Roelens, J. A. Bolger, D. Williams, and B. J. Eggleton, Opt. Express **16,** 10152 (2008).
9. T. Gong, F. Yan, D. Lu, M. Chen, P. Liu, P. Tao, M. Wang, T. Li, and S. Jian, Opt. Commun. **282,** 3460 (2009).
10. H. Weber, R. Ludwig, S. Ferber, C. Schmidt-Langhorst, M. Kroh, V. Marembert, C. Boerner, and C. Schubert, J. Lightwave Technol. **24,** 4616 (2006).
11. N. Jia, T. Li, K. Zhong, M. Wang, M. Chen, D. Lu, W. Peng, and J. Chi, Chin. Opt. Lett. **8,** 741 (2010).